arXiv:hep-ph/0207160v1 12 Jul 2002

# Bounds on Broken $R$-Parity from NOMAD and CHORUS

Herbi Dreiner[1]*, Giacomo Polesello[2]†, Marc Thormeier[3]‡

[1] *Physikalisches Institut der Universität Bonn, Nußallee 12, 53115 Bonn, Germany*

[2] *INFN, Sezione di Pavia, Via Bassi 6, 27100 Pavia, Italy*

[3] *Department of Theoretical Physics, University of Oxford, 1 Keble Road, Oxford OX1 3NP, United Kingdom*

**Abstract**

We determine new constraints on the products of two $R$-parity violating coupling constants from the NOMAD and CHORUS experiments on $\nu_\mu \to \nu_\tau$ oscillations. We obtain improved results from (a) lepton flavour violating (LFV) meson decays, (b) LFV deep-inelastic scattering and (c) a combination of the two.

## 1 Introduction

The superpotential of the *MSSM*+$\not{R}_p$ is obtained from the superpotential of the *MSSM* by adding the following terms (*c.f.* ref.[1])

$$\begin{aligned}\Delta\mathcal{W}_{\not{R}_p} &= \frac{1}{2}\varepsilon^{ab}\lambda_{ijk}\, L^i{}_a L^j{}_b E^{kC} + \varepsilon^{ab}\delta^{xy}\lambda'_{ijk}\, L^i{}_a Q^j{}_{bx} D^k{}_y{}^C \\ &\quad + \frac{1}{2}\,\varepsilon^{xyz}\lambda''_{ijk}\, U^i{}_x{}^C D^j{}_y{}^C D^k{}_z{}^C + \varepsilon^{ab}\kappa_i\, L^i{}_a H^{\mathcal{U}}{}_b. \end{aligned} \quad (1)$$

$H, Q, L$ represent the left chiral $SU(2)_W$-doublet superfields of the Higgses, the quarks and leptons; $U, D, E$ represent the right chiral superfields of the $u$-type quarks, $d$-type

*dreiner@th.physik.uni-bonn.de
†Giacomo.Polesello@pavia.infn.it
‡thor@thphys.ox.ac.uk

quarks and electron-type leptons $\ell$, respectively; a superscript $^C$ denotes charge conjugation; $a, b$ and $x, y, z$ are $SU(2)_W$ and $SU(3)_C$ indices; $i, j, k$ and later also $f, l, m$ are generation indices (summation over repeated indices is implied); $\delta^{xy}$ is the Kronecker symbol, $\varepsilon^{\cdots}$ symbolizes any tensor that is totally antisymmetric with respect to the exchange of any two indices, with $\varepsilon^{12\cdots} = 1$. The coupling constants $\lambda_{ijk}, \lambda''_{ijk}$ are antisymmetric with respect to the exchange of the first two/last two indices. The last term in eq.(1) can be rotated away utilizing a unitary field-redefinition [2].

Good agreement between the *SM* theory and experiment gives stringent upper bounds on the extra 45 coupling constants $\lambda_{ijk}, \lambda'_{ijk}$ and $\lambda''_{ijk}$, as well as on products thereof. For a list of references and the processes dealt with, see e.g. [3, 4, 5]. The first systematic analysis of $R\!\!\!/_p$ bounds was presented in [6], among other processes also utilizing neutrino deep-inelastic scattering. We look at this in considerably more detail here including also lepton flavour violating meson decays and including explicitly experimental effects. We also go beyond [6] to allow products of couplings.

Both processes can be tested by neutrino oscillation experiments. In this article we concentrate on the NOMAD [7] and CHORUS [8] experiments at CERN, for several reasons. These two experiments looked for muon-neutrinos oscillating to tau-neutrinos, thus addressing the products of couplings for second and third generation leptons, which are less constrained than the first generation. The limits obtained by these experiments are the most stringent to date, thanks to the high statistics running. Lastly, although the two experiments are dismantled, the two collaborations are still active, so the numerical factors (see below) which are necessary to extract firm limits and which are not available in the published literature can still be evaluated.

## 2 Lepton Flavour Violation at CHORUS & NOMAD

CERN's SPS fires a proton beam on a Beryllium target. From the resulting jet the secondary mesons (mostly pions and kaons) are charge selected and left to decay into mainly muons and neutrinos. After the neutrinos have propagated some distance they are indirectly detected via neutrino deep-inelastic scattering ($\nu$-DIS) on a nucleon in the target, producing a charged lepton plus other debris. The dominating *SM* process is

$$\begin{aligned} p + Be \implies (\pi^+ \text{ or } K^+) &\xrightarrow{SM} \mu^C + \nu_\mu \\ \nu_\mu &\xrightarrow{SM} \nu_\mu \\ \nu_\mu + N &\xrightarrow{SM} \mu^- + X, \end{aligned}$$

resulting in an isolated muon and a jet of many hadrons ($X$). We are interested in detecting deviations from the *SM* via lepton flavour violating interactions, in particular those resulting in a final state tau. Allowing for at most one non-*SM* process, we have the following possibilities[1]

$$
\begin{aligned}
(I) \qquad p + Be \implies (\pi^+ \text{ or } K^+) &\xrightarrow{\not{R}_p} \mu^C + \nu_\tau \\
\nu_\tau &\xrightarrow{SM} \nu_\tau \\
\nu_\tau + N &\xrightarrow{SM} \tau + X,
\end{aligned}
$$

$$
\begin{aligned}
(II) \qquad p + Be \implies (\pi^+ \text{ or } K^+) &\xrightarrow{SM} \mu^C + \nu_\mu \\
\nu_\mu &\xrightarrow{oscil.} \nu_\tau \\
\nu_\tau + N &\xrightarrow{SM} \tau + X,
\end{aligned}
$$

$$
\begin{aligned}
(III) \qquad p + Be \implies (\pi^+ \text{ or } K^+) &\xrightarrow{SM} \mu^C + \nu_\mu \\
\nu_\mu &\xrightarrow{SM} \nu_\mu \\
\nu_\mu + N &\xrightarrow{\not{R}_p} \tau + X.
\end{aligned}
$$

Here we focus on the cases $(I)$ and $(III)$, as well as the combination of $(I)$ and $(III)$. We do not further discuss $(II)$ since the case of neutrino oscillations has been treated extensively, see e.g. [10, 11]. A rough estimate of the case $(III)$ was made in [12], which mainly focuses on other issues. The detector efficiencies, the spectrum of the neutrino beam and the convolution of the partonic cross section with the parton distribution functions (pdf's) were not taken into account. In addition, the coupling considered in [12] also contributes to $(I)$ and the combined effect must be taken into account, as we do in section 6. Our bound is a factor 3.3 better.

We are interested in the theoretical prediction of the ratio of the number of tau-detections $\mathcal{N}_\tau$ over the number of muon-detections $\mathcal{N}_\mu$, to be compared with $\eta_{exp}$, the experimental upper bound on the number of tau-detections per muon-detection. The latter is given by CHORUS and NOMAD from their neutrino oscillation analysis, of which we make explicit use. We assume that the new physics does not significantly affect the muon detection rate and obtain

$$
\frac{\mathcal{N}_\tau}{\mathcal{N}_\mu} = \frac{\mathcal{N}_\tau^{\not{R}_p\text{-}decay} + \mathcal{N}_\tau^{oscil.} + \mathcal{N}_\tau^{\not{R}_p\text{-}DIS}}{\mathcal{N}_\mu^{SM} + \mathcal{N}_\mu^{\not{R}_p\text{-}decay} + \mathcal{N}_\mu^{oscil.} + \mathcal{N}_\mu^{\not{R}_p\text{-}DIS}} \approx \frac{\mathcal{N}_\tau^{\not{R}_p\text{-}decay} + \mathcal{N}_\tau^{oscil.} + \mathcal{N}_\tau^{\not{R}_p\text{-}DIS}}{\mathcal{N}_\mu^{SM}} \;\leq\; \eta_{exp}. \tag{2}
$$

[1] NOMAD and CHORUS are also sensitive to $R$-parity violation via late decaying neutralinos [9].

Here $\mathcal{N}_\ell^Y$ is the number of observed leptons $\ell$ which are due to the process $Y$. We shall here only analyze $\tau$'s which originate either from a $\not{R}_p$ meson decay or from $\not{R}_p$-DIS.

The probability that a $\tau$ is detected due to flavour violating $\nu$-DIS is given by

$$P_\sigma \;\equiv\; \widetilde{\chi}\cdot\frac{\sum\limits_{N=n,p}\mathbf{N}_N\sum\limits_{i=1}^{3}\sum\limits_{j=1}^{2}\left(\chi_{d^iu^j}\;\sigma^{\not{R}_p,\ all\ E_\nu}_{\nu_\mu+N_{d^i}\to\tau+X}\;+\;\chi_{u^jCd^iC}\;\sigma^{\not{R}_p,\ all\ E_\nu}_{\nu_\mu+N_{u^jC}\to\tau+X'}\right)}{\sum\limits_{N=n,p}\mathbf{N}_N\sum\limits_{i=1}^{3}\sum\limits_{j=1}^{2}\left(\sigma^{SM,\ all\ E_\nu}_{\nu_\mu+N_{d^i}\to\mu+X}\;+\;\sigma^{SM,\ all\ E_\nu}_{\nu_\mu+N_{u^jC}\to\mu+X'}\right)}\,. \qquad (3)$$

Here $P_\sigma = P_\sigma(\lambda'^*_{3jk}\lambda'_{2ik}, \lambda'^*_{kji}\lambda_{2k3})$. $\mathbf{N}_N$ is the number of the nucleon-type $N$ in the detector target and $\sigma$ denotes a cross section which has been integrated over the indicated parton distribution function *and* over the incoming neutrino energy distribution. The detector efficiency correction factors, $\widetilde{\chi}$ and $\chi_{q_{in}q_{out}}$, are different for each physical process,

$$\chi_{q_{in}q_{out}} = \frac{\epsilon^{\not{R}_p}_{\nu_\mu+N_{q_{in}}\to\tau+X_{q_{out}}}}{\epsilon^{SM}_{\nu_\tau+N_{q_{in}}\to\tau+X_{q_{out}}}}\,, \qquad \widetilde{\chi} = \frac{\sigma^{SM\quad all\ E_\nu}_{\nu_\mu+N_{q_{in}}\to\mu+X_{q_{out}}}}{\sigma^{SM\quad all\ E_\nu}_{\nu_\tau+N_{q_{in}}\to\tau+X_{q_{out}}}}\,. \qquad (4)$$

$\epsilon$ denotes the efficiency of detecting a tau-neutrino with the experimental cuts used in the selection analysis, for each respective process. The ratio of efficiencies needs to be determined case by case for each considered analysis by generating a sample of $\not{R}_p$ interactions and applying the experimental cuts on it. We work with the target being isoscalar, which is approximately correct for both experiments [7, 8]. Thus the factors $\mathbf{N}_N$ in eq.(3) can be taken outside the sums and cancel.

In order to analyze the lepton flavour violating meson decays we define the fractions

$$P_\pi(\lambda'^*_{31k}\lambda'_{21k}, \lambda'^*_{k11}\lambda_{3k2}) \;\equiv\; \frac{\Gamma^{\not{R}_p}_{\pi\to\mu^C\nu_\tau}}{\Gamma^{SM}_{\pi\to\mu^C\nu_\mu}+\Gamma^{\not{R}_p}_{\pi\to\mu^C\nu_\tau}} \approx \frac{\Gamma^{\not{R}_p}_{\pi\to\mu^C\nu_\tau}}{\Gamma^{SM}_{\pi\to\mu^C\nu_\mu}}, \qquad (5)$$

$$P_K(\lambda'^*_{32k}\lambda'_{21k}, \lambda'^*_{k12}\lambda_{3k2}) \;\equiv\; \frac{\Gamma^{\not{R}_p}_{K\to\mu^C\nu_\tau}}{\Gamma^{SM}_{K\to\mu^C\nu_\mu}+\Gamma^{\not{R}_p}_{K\to\mu^C\nu_\tau}} \approx \frac{\Gamma^{\not{R}_p}_{K\to\mu^C\nu_\tau}}{\Gamma^{SM}_{K\to\mu^C\nu_\mu}}\,. \qquad (6)$$

The denominators are dominated by the *SM* decay. For each decay mode we have explicitly indicated the possible relevant $\not{R}_p$ coupling constants.

Furthermore, $F_\pi$ is the fraction of tau-neutrino events having a pion as a parent meson which survive the cuts applied for the oscillation analysis. The corresponding fraction originating from kaon decays is denoted $F_K$ and to a good approximation $F_K = 1 - F_\pi$. Using eqs.(3-6) with the relevant $\not{R}_p$ coupling constants, and since the probabilities are small, we obtain from eq.(2)

$$F_\pi\cdot P_\pi(\lambda'^*_{31k}\lambda'_{21k}, \lambda'^*_{k11}\lambda_{3k2}) \;+\; \left(1-F_\pi\right)\cdot P_K(\lambda'^*_{32k}\lambda'_{21k}, \lambda'^*_{k12}\lambda_{3k2}) \;+$$
$$P_{oscil.} \;+\; P_\sigma(\lambda'^*_{3jk}\lambda'_{2ik}, \lambda'^*_{kji}\lambda_{2k3}) \;\leq\; \eta_{exp}\,, \qquad (7)$$

with $i,k = 1,2,3$ and $j = 1,2$. We assume that the three processes do not mutually cancel each other, and we can thus determine separate bounds. Furthermore, we assume

in turn that only two $\not{R}_p$ coupling constants are non-zero. We thus determine bounds on either the $\not{R}_p$ coupling constants of the meson decay (section 4),

$$F_\pi \cdot P_\pi(\lambda'^*_{k11}\lambda_{3k2}), \quad \Big(1 - F_\pi\Big) \cdot P_K(\lambda'^*_{k12}\lambda_{3k2}) \leq \eta_{exp}\,, \tag{8}$$

or the $\not{R}_p$ coupling constants of the $\nu$-DIS (section 5),

$$P_\sigma(\lambda'^*_{kji}\lambda_{2k3}), \quad P_\sigma(\lambda'^*_{31k}\lambda'_{22k}), \quad P_\sigma(\lambda'^*_{31k}\lambda'_{23k}), \quad P_\sigma(\lambda'^*_{32k}\lambda'_{22k}), \quad P_\sigma(\lambda'^*_{32k}\lambda'_{23k}) \leq \eta_{exp}\,. \tag{9}$$

There are two special cases where a combination of two $\not{R}_p$ coupling constants contribute to both lepton flavour violating meson decays and $\nu$-DIS. Since this is experimentally not distinguishable we then consider the combined effects, which also lead to an enhanced sensitivity (section 6)

$$F_\pi \cdot P_\pi(\lambda'^*_{31k}\lambda'_{21k}) + P_\sigma(\lambda'^*_{31k}\lambda'_{21k}), \quad \Big(1 - F_\pi\Big) \cdot P_K(\lambda'^*_{32k}\lambda'_{21k}) + P_\sigma(\lambda'^*_{32k}\lambda'_{21k}) \leq \eta_{exp}\,. \tag{10}$$

We do not discuss bounds on neutrino oscillation.

We first continue with a discussion of the NOMAD and CHORUS experiments. We then discuss the case of an anomalous meson decay in section 4, the $\nu$-DIS is treated in section 5, and the case with meson decay and $\nu$-DIS combined in section 6. In section 7 we give a brief summary. Note that throughout this article we present the bounds on the $\not{R}_p$ coupling constants in the mass eigenstate base, in order to avoid model dependent results, see ref.[13, 14]. For theoretical models which predict a hierarchy of $\not{R}_p$ coupling constants, which we implicitly make use of, see for example [15, 16].

# 3 NOMAD and CHORUS

The NOMAD and CHORUS experiments were designed to search for the oscillation of a muon-neutrino into a tau-neutrino through the detection of the charged current interaction

$$\nu_\tau + N \to \tau + X, \tag{11}$$

followed by the decay of the tau in the detector. The search was performed in the muon-neutrino beam of the CERN SPS, which provides an intense $\nu_\mu$ beam with an average neutrino energy of 27 GeV. With a fiducial mass in the ton range (770 kg for CHORUS, 2.7 Tons for NOMAD), and a number of protons on target of $\sim 5 \times 10^{19}$, over a data-taking period of four years, each experiment has collected on the order of $10^6$ charged current muon-neutrino events ($\nu_\mu^{CC}$). Once analysis efficiencies have been taken into account, this yields a sensitivity to the presence of tau-neutrinos in the muon-neutrino

beam at the level of about one part in $10^4$ per experiment. The two experiments have taken complementary strategies to the detection of tau decay products.

The ***N***eutrino ***O***scillation ***Ma***gnetic ***D***etector (NOMAD), described in detail in ref.[7], is based on an active target consisting of drift chambers immersed in a 0.4 T magnetic field. The target is followed by a set of specialized detectors designed to achieve an efficient identification of electrons and muons. This design allows to fully reconstruct the kinematics of the events, which is used to discriminate between tau decays occurring in the detector, and misidentified $\nu_\mu^{CC}$ and $\nu_e^{CC}$ interactions. A set of detailed analyzes which fully exploit the discrimination power of the event kinematics separately for each decay channel of the tau have enabled them to put a stringent limit on the muon-neutrino to tau-neutrino oscillation probability. The final NOMAD result at 90% CL is [17]

$$P_{oscil.}^{NOMAD} < 1.63 \times 10^{-4}. \tag{12}$$

The ***C***ERN ***H***ybrid ***O***scillation ***R***esearch Apparat***us*** (CHORUS), described in detail in ref.[8], uses a hybrid setup, with a target based on nuclear emulsions, followed by a spectrometer system and a calorimeter. This allows the measurement of the momentum of the particles emerging from the target region, and the identification of the muons.

The information of the electronic detectors is used to apply loose kinematic selections, which define the data sets on which to perform the tau search in the emulsion stack. The decay modes of the tau into a muon or a single hadron are identified by the detection of a *kink*, i.e. a track from the interaction vertex showing a change in direction after a short path, of the order of $\gamma c\tau_\tau = \mathcal{O}(1\,mm)$. The latest CHORUS results, based on the analysis of a fraction of the events, see ref.[18], give no candidate observed, yielding a limit:

$$P_{oscil.}^{CHORUS} < 3.4 \times 10^{-4}. \tag{13}$$

It should be noted that the CHORUS oscillation limit is obtained with a different statistical treatment than the NOMAD one. If the same treatment were applied, the CHORUS result would be roughly $P_{oscil.}^{CHORUS} < 2.1 \times 10^{-4}$, see ref.[19].

No official combined limit from the two experiments is available. An exercise of combining the results, based on the statistical techniques used in NOMAD [19] , yields

$$P_{oscil.}^{combined} < 5 \times 10^{-5}. \tag{14}$$

We thus use $\eta_{exp} = 5 \times 10^{-5}$.

The two experiments have also obtained limits on the electron-neutrinos oscillating to tau-neutrinos, based on the $\sim 1\%$ contamination of electron-neutrinos, in the muon-neutrino beam. The limits are about two orders of magnitude worse than the previously

discussed case, which is why we do not treat electron-neutrinos in this paper. The extension is however straightforward.

## 4 $(\pi^+ \text{ or } K^+) \xrightarrow{\not{R}_p} \mu^C + \nu_\tau$

Starting from eq.(8), the results in section 2.1 of ref.[20] lead to

$$\frac{\Gamma^{\not{R}_p}_{\pi\to\mu+\nu_\tau}}{\Gamma^{SM}_{\pi\to\mu+\nu_\mu}} = |K_{1123}|^2 \leq \frac{\eta_{exp}}{F_\pi}, \tag{15}$$

with

$$K_{1123} = \frac{-\ m_\pi^2}{2\sqrt{2}\ G_F\ |V_{11}|\ m_\mu(m_u+m_d)}\ \frac{\lambda'^*_{k11}\ \lambda_{3k2}}{m^2_{\widetilde{\ell_L}^k}}\,. \tag{16}$$

$G_F$ is the Fermi constant and $V_{ji}$ is an element of the CKM-matrix, $m$ symbolizes a mass. Here we have neglected the correction factors due to higher order electroweak leading logarithms, short distance *QCD* corrections, and structure dependent effects. The analogous constant to eq.(16) for kaon decay, $K_{2123}$ is obtained from $K_{1123}$ by replacing $m_\pi \to m_K$, $m_d \to m_s$ and $\lambda'^*_{k11}\ \lambda_{3k2} \to \lambda'^*_{k12}\lambda_{3k2}$.

With $G_F = (0.116639 \pm 0.000001) \times (100\ \text{GeV})^{-2}$, $m_\mu = (105.6583568 \pm 5.2 \times 10^{-6})$ MeV, $m_\pi = (139.57018 \pm 0.00035)$ MeV, $m_u + m_d = (8.5 \pm 3.5)$ MeV, $|V_{11}| = 0.9750 \pm 0.0008$, $m_K = (493.677 \pm 0.016)$ MeV, $m_s = (122.5 \pm 47.5)$ MeV, $m_s = (21 \pm 4)\ m_d$, and $|V_{12}| = 0.222 \pm 0.004$ [21], one gets, using central values,

$$|\lambda'^*_{k11}\lambda_{3k2}| \ \leq\ 0.014\sqrt{\frac{\eta_{exp}}{F_\pi}}\left(\frac{m_{\widetilde{\ell_L}^k}}{100\,\text{GeV}}\right)^2, \tag{17}$$

$$|\lambda'^*_{k12}\lambda_{3k2}| \ \leq\ 0.0039\sqrt{\frac{\eta_{exp}}{1-F_\pi}}\left(\frac{m_{\widetilde{\ell_L}^k}}{100\,\text{GeV}}\right)^2. \tag{18}$$

The value of $F_\pi$ cannot be evaluated with the published numbers. It is in fact a number which depends on the neutrino energy, and varies between $\sim 0$ for the lowest accessible neutrino energies to $\sim 1$ for the highest neutrino energy, as can be seen in Fig.1. This factor in turn needs to be convoluted with the efficiency of the analysis cuts at a given energy, which is also a function of the specific analysis.

The dependence on the neutrino energy of the global analysis efficiency for CHORUS is given in [18]. By convoluting the analysis efficiency with the different components of the neutrino spectra shown in Fig. 1, the approximate value for $F_\pi$ obtained in this way is $\sim 0.92$. We expect that the effective $F_\pi$ from the combination of the different analyses from NOMAD to be lower than this value. In fact CHORUS, for an equivalent limit on the oscillation probability, is able to exclude a significantly lower value of $\Delta m^2_\nu$, the difference of the mass squared of the two neutrino flavours [17, 18]. This means [21] that

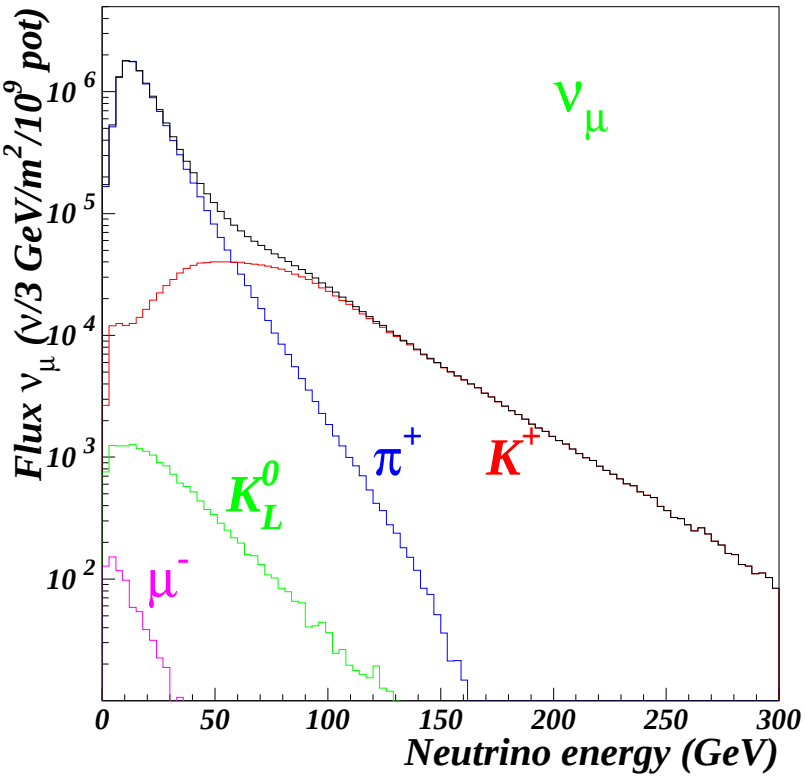


Figure 1: *Spectrum of the muon-neutrino beam at the NOMAD detector, from [22]. We show the muon neutrino flux originating from different particle decays. The two components of the neutrino spectrum, the one coming from pion and the other one coming from kaon decay, are separately shown on the graph.*

the average energy of the neutrinos surviving the analysis cuts is higher for NOMAD than for CHORUS. As can be seen from Fig. 1, a harder energy spectrum enhances the fraction of events for which the parent meson is a $K$. We extract a conservative limit from the available information by assuming that the NOMAD and CHORUS results contribute with a similar weight to the combined limit. For NOMAD we take $F_\pi$ varying between $\sim$0.1 and $\sim$0.9. The final range for the effective value of $F_\pi$ in our combined analysis is therefore:

$$0.5 \leq F_\pi \leq 0.9. \tag{19}$$

To be as conservative as possible we use the lower bound when dealing with the pion and the upper bound when dealing with the kaons. With eq.(14) we therefore obtain

$$\begin{aligned} |\lambda'^*_{211}\lambda_{322}| &\leq 1.4 \times 10^{-4} \left(\frac{m_{\widetilde{\ell_L}^k}}{100\ \text{GeV}}\right)^2, \\ |\lambda'^*_{k12}\lambda_{3k2}| &\leq 8.8 \times 10^{-5} \left(\frac{m_{\widetilde{\ell_L}^k}}{100\ \text{GeV}}\right)^2. \end{aligned} \tag{20}$$

Using the product of the bounds on single coupling constants [5], one gets a stricter bound on $|\lambda'^*_{111}\lambda_{312}|$ than we would obtain here.

## 5 $\nu_\mu + N \xrightarrow{\not R_p} \tau + X$

In order to determine a bound from $\nu$-DIS we must compute the cross section

$$\sigma^{all\ E_\nu}_{\nu_\mu + N_{q_{in}} \to \ell^f + X_{q_{out}}} = \int\limits_{E^{lab}_{\nu_\mu min}}^{E^{lab}_{\nu_\mu max}} \sigma_{\nu_\mu + N_{q_{in}} \to \ell^f + X_{q_{out}}}(s(E^{lab}_{\nu_\mu}))\ \ g(E^{lab}_{\nu_\mu})\ \ dE^{lab}_{\nu_\mu}\,, \tag{21}$$

for both the *SM* process ($f = 2$) and the $\not R_p$ process ($f = 3$). $g(E^{lab}_{\nu_\mu})$ is the incoming neutrino energy spectrum (in the lab frame) and is given in ref.[22]. $s \equiv (p_{\nu_\mu} + p_N)^2 = 2E^{lab}_{\nu_\mu} m_N + m_N^2$ is the center-of-mass energy. We perform the above integral numerically. The cross section in eq.(21) implicitly contains an integral over the quark distribution functions, which we discuss below. Explicitly in terms of the cross sections we have from eq.(9)

$$\frac{\widetilde{\chi}\ \sum\limits_{N,i,j}\ \int\limits_{E^{lab}_{\nu_\mu min}}^{E^{lab}_{\nu_\mu max}} g(E^{lab}_{\nu_\mu})\Big(\chi_{d^i u^j}\ \sigma^{\not R_p}_{\nu_\mu + N_{d^i} \to \tau + X_{u^j}}[s] + \chi_{u^j{}^C d^i{}^C}\ \sigma^{\not R_p}_{\nu_\mu + N_{u^j{}^C} \to \tau + X_{d^i{}^C}}[s]\Big)\ dE^{lab}_{\nu_\mu}}{\sum\limits_{N,i,j}\ \int\limits_{E^{lab}_{\nu_\mu min}}^{E^{lab}_{\nu_\mu max}} g(E^{lab}_{\nu_\mu})\Big(\sigma^{SM}_{\nu_\mu + N_{d^i} \to \mu + X_{u^j}}[s] + \sigma^{SM}_{\nu_\mu + N_{u^j{}^C} \to \mu + X_{d^i{}^C}}[s]\Big)\ dE^{lab}_{\nu_\mu}} \leq \eta_{exp}. \tag{22}$$

We calculate the cross sections for both the *SM* and the $\not R_p$ case by first computing the partonic cross sections $\sigma_{\nu_\mu + q_{in} \to \ell^f + q_{out}}$. With $\hat{s} \equiv (p_{\nu_\mu} + p_{q_{in}})^2$, and $t \equiv (p_{\nu_\mu} - p_{\ell^f})^2$ the averaged matrix elements squared in the *SM* are given by

$$\langle |\mathcal{M}_{\nu_\mu + d^i \xrightarrow{SM} \mu + u^j}|^2 \rangle = 16\ G_F^2\ |V_{ji}|^2\ (\hat{s} - m^2_{d^i})\ (\hat{s} - m^2_\mu - m^2_{u^j})\,, \tag{23}$$

$$\langle |\mathcal{M}_{\nu_\mu + u^j{}^C \xrightarrow{SM} \mu + d^i{}^C}|^2 \rangle = 16\ G_F^2\ |V_{ji}|^2\ (\hat{s} + t - m^2_{u^j} - m^2_\mu)\ (\hat{s} + t - m^2_{d^i})\,. \tag{24}$$

In the $\not R_p$ case, we obtain

$$\begin{aligned}
\langle |\mathcal{M}_{\nu_\mu + d^i \xrightarrow{\not R_p} \tau + u^j}|^2 \rangle &= \frac{1}{2}\left|\sum_k \frac{\lambda'^*_{3jk}\ \lambda'_{2ik}}{m^2_{\widetilde{d_R{}^k}}}\right|^2 (\hat{s} - m^2_{d^i})\ (\hat{s} - m^2_\tau - m^2_{u^j}) \\
&+ \mathrm{Re}\left[\left(\sum_k \frac{\lambda'^*_{3jk}\ \lambda'_{2ik}}{m^2_{\widetilde{d_R{}^k}}}\right)\cdot\left(\sum_k \frac{\lambda'^*_{kji}\ \lambda_{2k3}}{m^2_{\widetilde{\ell_L{}^k}}}\right)^*\right] m_{d^i}\ m_\tau\ (\hat{s} + t - m^2_\tau - m^2_{d^i}) \\
&+ \frac{1}{2}\left|\sum_k \frac{\lambda'^*_{kji}\ \lambda_{2k3}}{m^2_{\widetilde{\ell_L{}^k}}}\right|^2 (m^2_{d^i} + m^2_{u^j} - t)\ (m^2_\tau - t)\,,
\end{aligned} \tag{25}$$

$$\begin{aligned}
\langle |\mathcal{M}_{\nu_\mu + u^j{}^C \xrightarrow{\not R_p} \tau + d^i{}^C}|^2 \rangle &= \frac{1}{2}\left|\sum_k \frac{\lambda'^*_{3jk}\ \lambda'_{2ik}}{m^2_{\widetilde{d_R{}^k}}}\right|^2 (\hat{s} + t - m^2_\tau - m^2_{u^j})\ (\hat{s} + t - m^2_{d^i}) \\
&+ \mathrm{Re}\left[\left(\sum_k \frac{\lambda'^*_{3jk}\ \lambda'_{2ik}}{m^2_{\widetilde{d_R{}^k}}}\right)\cdot\left(\sum_k \frac{\lambda'^*_{kji}\ \lambda_{2k3}}{m^2_{\widetilde{\ell_L{}^k}}}\right)^*\right] m_{d^i}\ m_\tau\ (\hat{s} - m^2_{u^j}) \\
&+ \frac{1}{2}\left|\sum_k \frac{\lambda'^*_{kji}\ \lambda_{2k3}}{m^2_{\widetilde{\ell_L{}^k}}}\right|^2 (m^2_{d^i} + m^2_{u^j} - t)(m^2_\tau - t)\,.
\end{aligned} \tag{26}$$

$\langle ... \rangle$ denotes the average/sum over initial/final state spins. The differential cross section in the partonic CM-frame is given by

$$\frac{d\sigma_{\nu_\mu + q_{in} \to \ell f + q_{out}}}{d\cos\vartheta^{CM}} = \frac{\langle |\mathcal{M}_{\nu_\mu + q_{in} \to \ell f + q_{out}}|^2 \rangle \ |\vec{p}_{\ell f}|^{CM}}{32 \ \pi \ \hat{s} \ |\vec{p}_{\nu_\mu}|^{CM}} \,, \tag{27}$$

where $\vartheta^{CM}$ denotes the angle between the incoming neutrino and the outgoing charged lepton in the partonic CM-frame. In order to obtain the nuclear cross section we have to fold the partonic cross section with the pdf's $q_{in}^N(x,t)$

$$\sigma_{\nu_\mu + N_{q_{in}} \to \ell f + X_{q_{out}}}(s) = \int\limits_{x_{min}}^{x_{max}} \int\limits_{1}^{-1} \frac{d\sigma_{\nu_\mu + q_{in} \to \ell f + q_{out}}}{d\cos\vartheta^{CM}}(\hat{s},t) \ q_{in}^N(x,t) \ d\cos\vartheta^{CM} \ dx \,. \tag{28}$$

We use the pdf's given in ref.[23]. The Mandelstam variable $t$ is given by[2]

$$t = \frac{1}{2\hat{s}}\Big( (m_{\ell f}^2 + m_{q_{out}}^2 - \hat{s})\hat{s} + (m_{\ell f}^2 - m_{q_{out}}^2 + \hat{s}) m_{q_{in}}^2 + (\hat{s} - m_{q_{in}}^2)\cos\vartheta^{CM} \sqrt{...} \ \Big) \,. \tag{29}$$

and $\sqrt{...} \equiv \sqrt{m_{\ell f}^4 + (m_{q_{out}}^2 - \hat{s})^2 - 2 \ m_{\ell f}^2 (m_{q_{out}}^2 + \hat{s})}$. Furthermore $x$ is the Bjorken scaling variable, defined as $p_{q_{in}} = x p_N$. By definition $x_{max} = 1$. $x$ is given explicitly in terms of the momenta by

$$x = \frac{s - m_N^2}{2 \ m_N^2} \ \left[ \sqrt{1 + \Big( \frac{2(p_{\ell f} + p_{q_{out}}) \ m_N}{s - m_N^2} \Big)^2} \ - \ 1 \right] . \tag{30}$$

We obtain the minimum allowed value, $x_{min}$, when the outgoing fermions are at rest in the partonic CM-frame

$$x_{min} = \frac{s - m_N^2}{2 \ m_N^2} \ \left[ \sqrt{1 + \left( \frac{2(m_{\ell f} + m_{q_{out}}) \ m_N}{s - m_N^2} \right)^2} \ - \ 1 \right] . \tag{31}$$

For each matrix element squared in eqs.(23)-(26), we can compute the total cross section in eq.(28) using the differential cross section in eq.(27) as well as the formulæ of eqs.(29) through (31). The *SM* cross sections as well as the relevant $\not{R}_p$ cross section are then inserted in eq.(22) in order to obtain a bound on the $\not{R}_p$ coupling constants.

As stated above, we assume that in any given case only two $\not{R}_p$-couplings are non-zero. There are then no interference terms in the matrix elements squared given in eqs.(25) and (26) and the product of the couplings factor out of all the integrals. We thus directly obtain a bound on the product of the $\not{R}_p$ coupling constants considered.[3]

We determine explicit bounds with the following numerical values $m_c = (1250 \pm 100)$ MeV, $m_b = (4200 \pm 200)$ MeV, $m_\tau = (1776.99 \pm 0.29)$ MeV, $m_p = (938.271998 \pm 0.000038)$

[2]For the sake of generality we shall at the moment not work with $m_{q_{in}} = 0$, although it is required by the parton model.

[3]From now we work with $m_{q_{in}} = 0$, as required by the parton model.

MeV, $m_n = (939.565330 \pm 0.000038)$ MeV, $|V_{13}| = 0.0035 \pm 0.0015$, $|V_{21}| = 0.222 \pm 0.003$, $|V_{22}| = 0.941 \pm 0.008$, $|V_{23}| = 0.040 \pm 0.03$, [21]. We then obtain

$$|\lambda'^{*}_{k11}\ \lambda_{2k3}| \ \leq \ \frac{1}{\sqrt{0.43\ \chi_{du} + 0.036\ \chi_{u^C d^C}}}\ \times\ \sqrt{\frac{\eta_{exp}}{\widetilde{\chi}}}\ \left(\frac{m_{\widetilde{\ell_L^k}}}{100\ \mathrm{GeV}}\right)^2 . \tag{32}$$

The coefficients of the $\chi_{q_{in}q_{out}}$ depend on the pdf's and we determined them numerically. Thus each process listed in eq.(9) will have different coefficients. The other processes, however, do not lead to improved bounds beyond those published in the literature [5], as we discuss below. For completeness we list the corresponding set of equations in the appendix.

The factor $\widetilde{\chi}$ is 1/0.48 for the NOMAD DIS analyses and 1/0.53 for CHORUS (see ref.[17] and ref.[18]). We shall hence work with

$$\widetilde{\chi} = 2. \tag{33}$$

The standard model $\nu_\tau^{CC}$ cross section is dominated by $\nu_\tau d \to \tau^- u$. One can therefore make the simplifying assumption

$$\chi_{du} \sim 1\,. \tag{34}$$

There is no reliable estimate for the other quark combinations, $\chi_{q_{in}q_{out}}$. In fact the difference of the momentum distribution of the quarks in the nucleon, with respect to the valence $d$ quark, and/or the presence of heavy ($c$ or $b$) quarks in the final state significantly alters the kinematic distributions of the final state products. It would therefore be necessary to perform a detailed simulation of the experimental analysis to extract the efficiency values. Therefore, we only explicitly calculate the case (with $\chi_{u^C d^C} = 0$)

$$|\lambda'^{*}_{k11}\ \lambda_{2k3}| \leq 0.0076 \left(\frac{m_{\widetilde{\ell_L^k}}}{100\ \mathrm{GeV}}\right)^2 . \tag{35}$$

This is to be compared with the product of single coupling bounds summarized in ref.[5]. For $k = 1$ the product of single bounds is significantly stricter. $k = 2$ is not allowed due to the anti-symmetry in the $LLE^C$ operators. For $k = 3$ the product of single coupling bounds is virtually identical to the above bound. However, there the bound on $\lambda'_{311}$ depends on the squark mass $m_{\widetilde{d_R}}$ and the bound on $\lambda_{233}$ depends on the right handed slepton mass. If $m_{\widetilde{d_R}} \gg m_{\widetilde{\tau_L}}$, our bound will be the best bound.

The next most promising case for an additional new limit is $\lambda'^{*}_{k21}\lambda_{2k3}$, with an in-going valence $d$-quark and an out-going charm quark. Although we cannot quantify $\chi_{dc}$, we can evaluate the limit under optimistic assumptions. For $\chi_{dc} = 1$ and $\chi_{c^C d^C} = 0$ we obtain

$$|\lambda'^{*}_{k21}\lambda_{2k3}| \lesssim 0.006 \left(\frac{m_{\widetilde{\ell_L^k}}}{100\ \mathrm{GeV}}\right)^2 . \tag{36}$$

This is comparable to the product of the single couplings limits for $k = 1$, which is 0.002 and somewhat better for $k = 3$: 0.035. The bounds on the other products are not competitive. In the appendix we have summarized the formulæ for the bounds from $\nu$-DIS, explicitly retaining $\chi_{q_{in}q_{out}}, \eta_{exp}, \widetilde{\chi}$.

# 6 $(\pi^+$ or $K^+) \xrightarrow{\not{R}_p} \mu^C + \nu_\tau$ combined with $\nu_\mu + N \xrightarrow{\not{R}_p} \tau + X$

Here we use eq.(10), i.e. we combine DIS and meson decays. For the DIS analysis we use eq.(34). For the meson decays we again make use of the results stated in ref.[20] section 2.1. The conservative approach we follow is to set $F_\pi$ to the smallest value in the established range for each of the expressions stated below, and furthermore to set $\chi_{u^C d^C} = \chi_{dc} = \chi_{c^C d^C} = 0$. We obtain the limits

$$\begin{aligned} |\lambda'^{*}_{31k}\ \lambda'_{21k}| &\leq \frac{0.117\ \sqrt{32\ \eta_{exp}}}{\sqrt{\frac{F_\pi}{|V_{11}|^2} + \widetilde{\chi}(0.49\ \chi_{du} + 0.012\ \chi_{u^C d^C})}} \left(\frac{m_{\widetilde{d^k_R}}}{100\ \text{GeV}}\right)^2 \\ &= 0.0038 \left(\frac{m_{\widetilde{d^k_R}}}{100\ \text{GeV}}\right)^2, \end{aligned} \tag{37}$$

$$\begin{aligned} |\lambda'^{*}_{32k}\ \lambda'_{21k}| &\leq \frac{0.117\ \sqrt{32\ \eta_{exp}}}{\sqrt{\frac{1-F_\pi}{|V_{12}|^2} + \widetilde{\chi}(0.43\ \chi_{dc} + 0.0015\ \chi_{c^C d^C})}} \left(\frac{m_{\widetilde{d^k_R}}}{100\ \text{GeV}}\right)^2 \\ &= 0.0027 \left(\frac{m_{\widetilde{d^k_R}}}{100\ \text{GeV}}\right)^2. \end{aligned} \tag{38}$$

Note that in the second case we combined $K^+ \to \mu^C + \nu_\tau$ with $\nu_\mu + d \to \tau + c \big/ \nu_\mu + c^C \to \tau + d^C$. Both bounds are improvements compared to products of bounds on single coupling constants: respectively 0.0064 and 0.031 [5].

# 7 Summary and Conclusion

We have investigated the bounds that can be obtained on the product of $R$-parity violating coupling constants by employing the neutrino oscillation analyses of the NOMAD and CHORUS experiments. They are sensitive to lepton number violating meson decays leading to tau neutrinos and to neutrino deep inelastic scattering in which tau leptons are produced in the final state. We obtain the following bounds which are more sensitive than the product of existing single coupling bounds, and thus present the best bounds on these coupling constant combinations

$$|\lambda'^{*}_{211}\ \lambda_{322}| \leq 1.4 \times 10^{-4} \left(\frac{m_{\widetilde{\ell^2_L}}}{100\ \text{GeV}}\right)^2, \tag{39}$$

$$|\lambda'^{*}_{k12}\ \lambda_{3k2}| \ \leq \ 8.8\times 10^{-5}\left(\frac{m_{\widetilde{\ell_L}^k}}{100\ \mathrm{GeV}}\right)^2, \tag{40}$$

$$|\lambda'^{*}_{31k}\ \lambda'_{21k}| \ \leq \ 3.8\times 10^{-3}\left(\frac{m_{\widetilde{d_R}^2}}{100\ \mathrm{GeV}}\right)^2, \tag{41}$$

$$|\lambda'^{*}_{32k}\ \lambda'_{21k}| \ \leq \ 2.7\ \times 10^{-3}\left(\frac{m_{\widetilde{d_R}^k}}{100\ \mathrm{GeV}}\right)^2. \tag{42}$$

For completeness we list the formulæ for all processes corresponding to eq.(32) in the appendix. Even for optimistic estimates of the efficiencies, the resulting bounds are weaker than existing bounds or only a marginal improvement.

# 8 Acknowledgments

We thank Ulrich Langenfeld for useful discussions on numerical computing and Dick Roberts for valuable advice on MRST2001. We thank Roberto Petti for enlightening discussions on the NOMAD results. M.T. gratefully acknowledges the kind hospitality of the Physikalisches Institut at Universität Bonn, and the financial support of the Evangelisches Studienwerk and Worcester College, Oxford.

# Appendix

From $\nu$-DIS we obtain the following bounds, explicitly retaining $\chi_{q_{in}q_{out}}, \eta_{exp}, \widetilde{\chi}$:

$$|\lambda'^{*}_{31k}\ \lambda'_{22k}| \ \leq \ \frac{1}{\sqrt{0.055\ \chi_{su}+0.028\ \chi_{u^Cs^C}}}\ \times\ \sqrt{\frac{\eta_{exp}}{\widetilde{\chi}}}\ \left(\frac{m_{\widetilde{d_R}^k}}{100\ \mathrm{GeV}}\right)^2,$$

$$|\lambda'^{*}_{31k}\ \lambda'_{23k}| \ \leq \ \frac{1}{\sqrt{0.00052\ \chi_{bu}+0.0024\ \chi_{u^Cb^C}}}\ \times\ \sqrt{\frac{\eta_{exp}}{\widetilde{\chi}}}\ \left(\frac{m_{\widetilde{d_R}^k}}{100\ \mathrm{GeV}}\right)^2,$$

$$|\lambda'^{*}_{32k}\ \lambda'_{22k}| \ \leq \ \frac{1}{\sqrt{0.047\ \chi_{sc}+0.0036\ \chi_{c^Cs^C}}}\ \times\ \sqrt{\frac{\eta_{exp}}{\widetilde{\chi}}}\ \left(\frac{m_{\widetilde{d_R}^k}}{100\ \mathrm{GeV}}\right)^2,$$

$$|\lambda'^{*}_{32k}\ \lambda'_{23k}| \ \leq \ \frac{1}{\sqrt{0.00051\ \chi_{bc}+0.00039\ \chi_{c^Cb^C}}}\ \times\ \sqrt{\frac{\eta_{exp}}{\widetilde{\chi}}}\ \left(\frac{m_{\widetilde{d_R}^k}}{100\ \mathrm{GeV}}\right)^2,$$

$$|\lambda'^{*}_{k11}\ \lambda_{2k3}| \ \leq \ \frac{1}{\sqrt{0.43\ \chi_{du}+0.036\ \chi_{u^Cd^C}}}\ \times\ \sqrt{\frac{\eta_{exp}}{\widetilde{\chi}}}\ \left(\frac{m_{\widetilde{\ell_L}^k}}{100\ \mathrm{GeV}}\right)^2,$$

$$|\lambda'^{*}_{k12}\ \lambda_{2k3}| \ \leq \ \frac{1}{\sqrt{0.023\ \chi_{su}+0.036\ \chi_{u^Cs^C}}}\ \times\ \sqrt{\frac{\eta_{exp}}{\widetilde{\chi}}}\ \left(\frac{m_{\widetilde{\ell_L}^k}}{100\ \mathrm{GeV}}\right)^2,$$

$$|\lambda'^{*}_{k13}\ \lambda_{2k3}| \ \leq \ \frac{1}{\sqrt{0.00010\ \chi_{bu}+0.0020\ \chi_{u^Cb^C}}}\ \times\ \sqrt{\frac{\eta_{exp}}{\widetilde{\chi}}}\left(\frac{m_{\widetilde{\ell_L}^k}}{100\ \mathrm{GeV}}\right)^2,$$

$$|\lambda'^{*}_{k21}\ \lambda_{2k3}| \ \leq \ \frac{1}{\sqrt{0.52\ \chi_{dc} + 0.0068\ \chi_{c^C d^C}}} \ \times \ \sqrt{\frac{\eta_{exp}}{\widetilde{\chi}}} \left(\frac{m_{\widetilde{\ell_L}^k}}{100\ \mathrm{GeV}}\right)^2,$$

$$|\lambda'^{*}_{k22}\ \lambda_{2k3}| \ \leq \ \frac{1}{\sqrt{0.030\ \chi_{sc} + 0.0068\ \chi_{c^C s^C}}} \ \times \ \sqrt{\frac{\eta_{exp}}{\widetilde{\chi}}} \left(\frac{m_{\widetilde{\ell_L}^k}}{100\ \mathrm{GeV}}\right)^2,$$

$$|\lambda'^{*}_{k23}\ \lambda_{2k3}| \ \leq \ \frac{1}{\sqrt{0.00011\ \chi_{bc} + 0.00042\ \chi_{c^C b^C}}} \ \times \ \sqrt{\frac{\eta_{exp}}{\widetilde{\chi}}} \left(\frac{m_{\widetilde{\ell_L}^k}}{100\ \mathrm{GeV}}\right)^2.$$

# References


[1] S.Weinberg, *Phys.Rev.* **D26** 287 (1982).

[2] L.Hall, M.Suzuki, *Nucl.Phys.* **B231** 419 (1984).

[3] H.Dreiner, *hep-ph/9707435*.

[4] G.Bhattacharyya, *Nucl.Phys.Proc.Suppl.* **52A** 83 (1997); *hep-ph/9608415*.

[5] B.Allanach, A.Dedes, H.Dreiner, *Phys.Rev.* **D60** 075014 (1999); *hep-ph/9906209*.

[6] V.Barger, G.Giudice, T.Han, *Phys.Rev.* **D40** 2987 (1989).

[7] NOMAD Collaboration, J.Altegoer et al., *Nucl.Instrum. Methods* **A404** 96 (1998).

[8] CHORUS Collaboration, E.Eskut et al., *Nucl.Instrum. Methods* **A401** 7 (1997).

[9] A.Dedes, H.Dreiner, P.Richardson, *Phys.Rev.* **D65** 015001 (2002); *hep-ph/0106199*.

[10] CHORUS Collaboration, E.Pesen, *Nucl.Phys.Proc.Suppl.* **70** 219 (1999).

[11] NOMAD Collaboration, P.Astier et al., *Phys.Lett.* **B453** 169 (1999).

[12] S.Gninenko, M.Kirsanov, N.Krasnikov, V.Matveev, *hep-ph/0106302*.

[13] K.Agashe, M.Graesser, *Phys.Rev.* **D54** 4445 (1996); *hep-ph/9510439*.

[14] H.Dreiner, P.Morawitz, *Nucl.Phys.* **B503** 55 (1997); *hep-ph/9703279*.

[15] P.Binétruy, S.Lavignac, P.Ramond, *Nucl.Phys.* **B477** 353 (1996); *hep-ph/9601243*.

[16] A.Chamseddine, H.Dreiner, *Nucl.Phys.* **B458** 65 (1996); *hep-ph/9504337*.

[17] NOMAD Collaboration, P.Astier et al., *Nucl.Phys.* **B611** 3 (2001); *hep-ex/0106102*.

[18] CHORUS Collaboration, E.Eskut et al., *Phys.Lett.* **B497** 8 (2001).

[19] R.Petti, Seminar given at DESY, March 2002, unpublished.

[20] H.Dreiner, G.Polesello, M.Thormeier; to appear in *Phys.Rev.* **D**; *hep-ph/0112228*.

[21] Particle Data Group, D.Groom et al., *Eur.Phys.J.* **C15** 1 (2000).
We have taken into account the update from Dec.12, 2001.

[22] G.Collazuol, A.Ferrari, A.Guglielmi, P.Sala, *Nucl.Instrum. Methods* **A449** 609 (2000).

[23] A.Martin, R.Roberts, W.Stirling, R.Thorne; *hep-ph/0110215*.